THE JOURNAL OF BIOLOGICAL CHEMISTRY
Vol. 278, No. 26, Issue of June 27, pp. 24053–24061, 2003

Printed in U.S.A.

How FMN Binds to *Anabaena* Apoflavodoxin

A HYDROPHOBIC ENCOUNTER AT AN OPEN BINDING SITE*

Received for publication, January 30, 2003, and in revised form, March 28, 2003
Published, JBC Papers in Press, April 7, 2003, DOI 10.1074/jbc.M301049200

Anabel Lostao‡, Fatna Daoudi‡, María Pilar Irún‡, Álvaro Ramón§, Concha Fernández-Cabrera§, Antonio Romero§, and Javier Sancho‡¶

From the ‡Departamento de Bioquímica y Biología Molecular y Celular, Facultad de Ciencias and Biocomputation and Complex Systems Physics Institute, Universidad de Zaragoza 50009-Zaragoza and §Centro de Investigaciones Biológicas, Consejo Superior de Investigaciones Científicas, Velázquez, 144 28006-Madrid, Spain

Molecular recognition begins when two molecules approach and establish interactions of certain strength. The mechanisms of molecular recognition reactions between biological molecules are not well known, and few systems have been analyzed in detail. We investigate here the reaction between an apoprotein and its physiological cofactor (apoflavodoxin and flavin mononucleotide) that binds reversibly to form a non-covalent complex (flavodoxin) involved in electron transfer reactions. We have analyzed the fast binding reactions between the FMN cofactor (and shorter analogs) and wild type (and nine mutant apoflavodoxins where residues interacting with FMN in the final complex have been replaced). The x-ray structures of two such mutants are reported that show the mutations are well tolerated by the protein. From the calculated microscopic binding rate constants we have performed a Φ analysis of the transition state of complex formation that indicates that the binding starts by interaction of the isoalloxazine-fused rings in FMN with residues of its hydrophobic binding site. In contrast, the phosphate in FMN, known to contribute most to the affinity of the final holoflavodoxin complex, is not bound in the transition state complex. Both the effects of ionic strength and of phosphate concentration on the wild type complex rate constant agree with this scenario. As suggested previously by nmr data, it seems that the isoalloxazine-binding site may be substantially open in solution. Interestingly, although FMN is a charged molecule, electrostatic interactions seem not to play a role in directing the binding, unlike what has been reported for other biological complexes. The binding can thus be best described as a hydrophobic encounter at an open binding site.

The active form of many proteins is a non-covalent complex between a polypeptide (the apoprotein) and a cofactor. Most flavoproteins are in this category (1). Among them, flavodoxins have been widely used to quantitate the energetics of apoprotein-cofactor complexes (2–7) because they can be conveniently overexpressed, deprived from the FMN cofactor, and reconstituted. Studies carried out on several flavodoxins indicate that a large part of the binding energy derives from interactions of the phosphate moiety of FMN with hydrogen donors situated at the N terminus of the first α-helix (Fig. 1). The isoalloxazine, redox, fused ring, sandwiched between aromatic residues in the complex, is the second binding energy spot of the cofactor, whereas the ribityl hardly contributes to stabilize the complex (7).

The strength of a complex derives, in the end, from a balance between the rate constants of binding and dissociation. Although the association of small molecules may be governed by the rates of diffusion in the solvent (8), where large molecules such as proteins are involved, significantly slower rates of association are typical because the molecular encounters often occur in inappropriate orientations (9, 10). In many cases, particularly in protein-protein complexes, a non-native complex is invoked to be formed initially, before the rate-limiting step takes place (11). Acceleration of binding reactions can be achieved if the interacting molecules can attract each other so that the diffusion limit is overcome or the approaching orientation is optimized. As the chief long distance attractive forces are electrostatic, acceleration of binding rates is often ascribed to electrostatic attraction between ligand and protein-binding site (12–14). In this respect, acceleration of the binding rate constant of a protein-protein complex without alteration of its dissociation rate constant has been engineered, giving rise to an increase in binding energy (15). Clearly, our understanding of the stability of functional complexes and our ability to modulate it when required is expected to benefit from a deeper comprehension of the mechanisms driving binding and dissociation.

Flavodoxin is an interesting model to investigate the mechanism of protein/ligand association. Among the flavodoxins that from *Anabaena* is particularly well suited because both the holo and apo x-ray structures are available (Fig. 1 and Ref. 16), and in addition, an extensive characterization of the solution behavior of the two forms has been performed (7, 17–24). The binding of FMN to apoflavodoxins from several species seems to occur in one step (5, 25), although the molecular details are not known. The flavin cofactor contains a charged phosphate moiety that could in principle facilitate an electrostatic orientation and approximation to the apoflavodoxin-binding site. In fact, inspection of the x-ray structure of the apoflavodoxin from *Anabaena* (17) indicates that the phosphate-binding site is well formed, whereas the isoalloxazine pocket is closed by one of the aromatic residues interacting with FMN in the functional complex (Trp^{57}). It is thus tempting to speculate that the binding of FMN starts by association at the phosphate-binding site. Conflicting with this hypothesis, solution studies on the structure of the *Anabaena* (20) and

* This work was supported by Grants BCM2001-252 from the Dirección General de Investigación and P120/2001 from the Diputación General de Aragón. The costs of publication of this article were defrayed in part by the payment of page charges. This article must therefore be hereby marked "*advertisement*" in accordance with 18 U.S.C. Section 1734 solely to indicate this fact.

The atomic coordinates and structure factors (code 1obo and 1obv) have been deposited in the Protein Data Bank, Research Collaboratory for Structural Bioinformatics, Rutgers University, New Brunswick, NJ (http://www.rcsb.org/).

¶ To whom correspondence should be addressed. Tel.: 34-976761286; Fax: 34-976762123; E-mail: jsancho@posta.unizar.es.

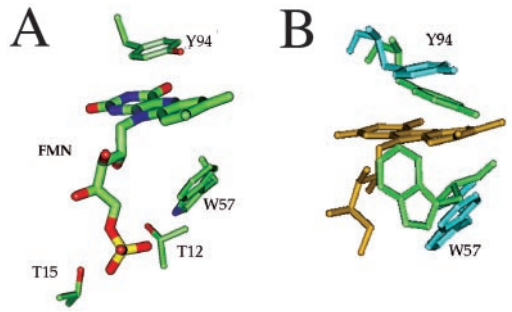

FIG. 1. **Views of the FMN-binding site in *Anabaena* flavodoxin (Protein Data Bank code 1flv) and in the apo form (Protein Data Bank code 1ftg).** *A*, environment of the FMN cofactor showing the binding site residues mutated (Thr^{12}, Thr^{15}, Trp^{57}, and Tyr^{94}). *B*, observed closure of the isoalloxazine-binding site in the apoflavodoxin (*green*) relative to the holo form (*blue*). The FMN bound in the holo form is shown in *gold*.

Azotobacter (26) apoflavodoxins suggest that the isoalloxazine-binding site is very flexible. This flexibility is also evidenced by the different x-ray structures observed for the Trp^{57} loop in wild type and mutant *Anabaena* flavodoxins (7). In addition, it should be noticed that the x-ray structure of *Anabaena* apoflavodoxin with the preformed phosphate-binding site bears a bound sulfate anion (17), which might be responsible for the observed local folding of the region. Thus, a different binding scenario, inspired by the structural evidence in solution, is one of binding at an opened isoalloxazine-binding site. We explore here the two possibilities by investigating the binding kinetics of FMN (and its shortened analogue, riboflavin) to wild type *Anabaena* apoflavodoxin and to mutants involving the two aromatic residues (Trp^{57} and Tyr^{94}) that sandwich the isoalloxazine ring (the x-ray structures of two such mutants is reported) and the two threonines at the phosphate-binding site (Thr^{12} and Thr^{15}). Determination of a low resolution structure for the transition state of complex formation by Φ analysis (27) of mutant binding rate constants together with the observed influence of the ionic strength and phosphate concentration on the binding kinetics allow us to discriminate between the two proposed binding scenarios.

EXPERIMENTAL PROCEDURES

Site-directed Mutagenesis—The mutant flavodoxins used in this work (W57Y, W57F, W57L, W57A, Y94W, Y94F, Y94L, and Y94A (19) and T12V and T15V (7)) have been prepared by oligonucleotide-directed mutagenesis of the *Anabaena* PCC 7119 flavodoxin gene, cloned in *Escherichia coli* (28), by using the method of Deng and Nickoloff (29) as implemented in the Transformer™ kit (2nd version) from Clontech.

Expression, Purification, and Protein Quantitation—The expression and purification of flavodoxin mutants were essentially as described previously (18). Apoflavodoxins were prepared by treatment with 3% trichloroacetic acid (2), followed by dialysis and ion-exchange fast protein liquid chromatography. The purity of each flavodoxin preparation was confirmed by SDS-PAGE. The concentration of mutant apoflavodoxins in solution was determined using an extinction coefficient calculated from the total amount of tyrosine and tryptophan residues in the protein (30). The concentration of wild type apoflavodoxin was determined using the extinction coefficient of 34.1 mM^{-1} cm^{-1} (18), very similar to the theoretical one calculated according to Gill and von Hippel (30).

Crystallization, Data Collection, Structure Solution, and Refinement—Initial crystallization trials were performed using the sitting-drop vapor diffusion method at 295 K. The search for suitable crystallization conditions was conducted with 96-condition Hampton Screens 1 and 2 (31) with drops assembled using 1 μl of protein (10 mg/ml) and 1 μl of reservoir solutions. The two mutant crystals (W57L and Y94F) appeared as clusters of rectangular cross-section rods growing from a common nucleation site, from solutions containing ammonium sulfate. These twinned crystals were not suitable for x-ray diffraction experiments. Attempts to improve the quality of the crystals were performed using a fine grid screen for ammonium sulfate concentrations (3–3.5 M) and varying the pH of the solutions using the counter-diffusion method on agarose gels (32). Crystals of W57L flavodoxin were grown from 3.5 M ammonium sulfate buffered with 0.1 M MES,[1] pH 6.0. The Y94F crystals were grown from 3.2 M ammonium sulfate buffered with 0.1 M Tris-HCl, pH 7.5. Both mutant crystals required a few weeks to a few months to grow to a suitable size for diffraction measurements. The largest rod had maximum dimensions of 0.3 × 0.3 × 0.2 mm.

For the diffraction experiments, crystals were flash-frozen in a stream of nitrogen gas at 100 K. The crystallization solution, mixed with 25% glycerol, was used as cryoprotectant. Data were collected for W57L with a Marccd detector at the DESY-X11 and for Y94F using a MAR image plate scanner in X31 beamlines at Hamburg, Germany. Data were processed with MOSFLM and SCALA of the CCP4 suite (33). For the high resolution W57L mutant, the 1.2-Å resolution assigned to the structure reflects the $I/\sigma(I) = 3.8$. To our knowledge, the W57L mutant diffracted to a higher resolution than any previously examined flavodoxin. The data collection statistics are presented in Table I.

The Y94F and W57L mutant structures were solved using molecular replacement methods. The oxidized structure of long chain flavodoxin from *Anabaena* (Ref. 16; Protein Data Bank code 1FLV) was used as the search model. The AMoRe system of programs (34) was used to complete the rotation and translation search as well as to apply the resulting values.

FMN Purification—FMN from wild type and mutant flavodoxins was purified to >99% by high pressure liquid chromatography using a C-18 column (from Vydac) and a methanol gradient (0–30%) in 5 mM ammonium acetate, pH 7.0. In addition, FMN from Sigma was purified to >95% following the same procedure.

Rate Constants of Flavin Binding—Rapid kinetics were performed and analyzed using an Applied Photophysics SX17.MV stopped-flow spectrofluorometer interfaced with an Acorn 5000 computer. Rate constants for flavin binding were determined from reaction of flavin with apoflavodoxin under pseudo first-order conditions (excess flavin), using the quenching of flavin fluorescence to monitor flavin binding. The concentration of apoprotein in the binding mixture was 0.5 μM for the complexes with FMN, 1.0 μM for the wild type apoflavodoxin-riboflavin complex, and 2.5 μM for the mutant apoflavodoxin complexes with riboflavin. Absorption spectra were recorded after each determination to calculate precisely the concentration of each reactant. Reactions were usually carried out in 50 mM MOPS, pH 7.0. In some experiments, NaCl was added to study the influence of ionic strength on the binding rate. To study the influence of phosphate concentration on the formation of the wild type flavodoxin complexes, a 50 mM MOPS, pH 7.0, buffer containing NaCl and sodium phosphate at a constant ionic strength of 500 mM was used. Rate constants as a function of temperature (from 5 to 43 °C) for the wild type apoflavodoxin-FMN complex were obtained by reaction of 0.5 μM wild type apoflavodoxin with 50 μM FMN in 50 mM MOPS, pH 7.0.

RESULTS

X-ray Structures of the W57L and Y94F Holoflavodoxins—The structures of the W57L and Y94F *Anabaena* flavodoxin mutants were determined from data collected at 100 K using synchrotron radiation at a 1.2- and 2.1-Å resolution, respectively. The folding shows clearly the α/β topology of this class of proteins, a five-stranded parallel β-sheet flanked by α-helices at either side. The analysis of the secondary structure shows that the three-dimensional structures of the mutants are essentially superimposable with that of the wt protein (not shown). Indeed, the bulk of the folding did remain the same in each mutant when compared with the wt holoflavodoxin, including the loop bearing residue 57, which seems quite flexible in apoflavodoxin (7). However, the hydrogen bonding network around the FMN is slightly different. The high resolution data collected for the W57L mutant allow the analysis of a detailed electron density map, partly shown in Fig. 2*A*, in which the atom positions of the flavin ring are clearly delineated. The FMN cofactor is tightly but non-covalently bound to the protein and is well defined (average B-factor = 8.3 $Å^2$). Table II shows the FMN group interactions to neighboring protein atoms of flavodoxin in the wild type (16) and the two mutant structures.

[1] The abbreviations used are: MES, 4-morpholineethanesulfonic acid; MOPS, 4-morpholinepropanesulfonic acid; wt, wild type.

TABLE I
Data collection and refinement statistics

	W57L	Y94F
Data collection statistics		
Space group	$P2_1$	$P2_12_12_1$
Cell dimensions (Å)	a = 37.63, b = 73.10, c = 57.05 β = 102.58	a = 44.08, b = 57.15, c = 58.93
No. molecules/asymmetry unit	2	1
Wavelength (Å)	0.9102	1.0489
Resolution (Å)	30–1.2	35–1.90
Measurements[a]	200,831 (28,242)	111,376 (11,740)
Unique reflections[a]	81,435 (11,496)	12,015 (1,138)
R_{sym} (%)[a]	3.8 (13.9)	6.0 (18.2)
$I/\sigma(I)$[a]	10.6 (3.6)	18.4 (2.6)
Completeness (%)[a]	94.7 (92.1)	98.0 (96.2)
Refinement statistics		
Resolution range (Å)	20–1.2	15–2.1
Reflections (work/free)	83,439/5,364	8,026/965
R_{work}/R_{free} (%)	18.6/20.3	18.8/24.7
Root mean square deviations from ideal geometry		
Bond lengths (Å)	0.005	0.007
Bond angles (°)	1.3	1.5
Dihedral angles (°)	22.9	23.8
e.s.d. for all atoms[b] (Å)	0.04[c]	0.06[d]
No. of atoms		
Protein	2650	1330
FMN	62	31
Solvent	341	145
Average B factor (Å^2)	10.6	15.7

[a] Values in parentheses correspond to the highest resolution shell.
[b] e.s.d., estimated standard deviations
[c] Estimated standard deviation from inversion of the full positional least squares matrix (54).
[d] Estimated standard deviation from SIGMAA (55).

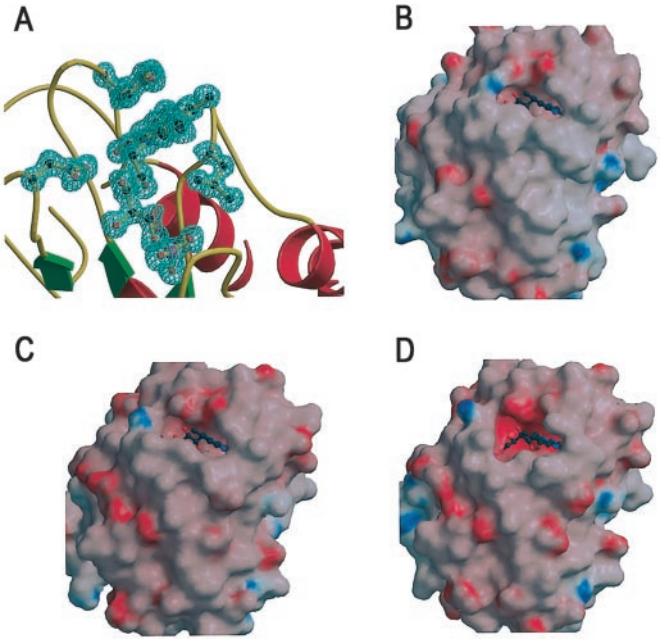

FIG. 2. **Electron density map of the FMN-binding site in W57L holoflavodoxin (*A*) and molecular surfaces of wild type (Protein Data Bank code 1flv, *B*), Y94F (*C*), and W57L (*D*) mutant holoflavodoxins.** The electron density map includes the FMN and its Leu^{57} and Tyr^{94} sandwiching groups. The molecular surfaces are colored to show the electrostatic potential and allow a visual evaluation of the solvent exposure of the bound FMN group (shown in *ball* and *stick*).

TABLE II
Interactions at the FMN-binding site

FMN atoms	Protein atoms	Distance		
		W57L	Y94F	Wild type[a]
N3	O Asn^{97}	2.87	2.82	2.92
O2	NH Gln^{99}	3.16	2.94	3.22
O4	NH Gly^{60}	2.77	2.78	2.86
O2′	O Thr^{56}	2.79	2.70	2.70
O3′	O$^{\delta2}$ Asp^{146}	2.60	2.63	2.65
	Nζ Lys^{14}			3.31
O5′	O$^{\gamma1}$ Thr^{88}		2.90	3.20
OP1	NH Thr^{12}	3.27	2.86	3.27
	NH Gly^{13}	3.18	3.12	3.16
	NH Lys^{14}	2.82	3.01	2.82
	O$^{\gamma1}$ Thr^{12}			2.64
OP2	NH Gln^{11}	2.99	2.80	2.81
	NH Thr^{12}	3.12	3.34	3.06
OP3	NH Thr^{15}	2.86	2.75	2.78
	O$^{\gamma1}$ Thr^{15}	2.64	3.07	2.65

[a] From Ref. 16.

Only the hydrogen bonds with favorable geometry have been taken into account. Most of the interactions are similar to those in other flavodoxin structures (16, 35–39). The phosphate group establishes O NH hydrogen bonds to residues of the N terminus of helix 1 (Gln^{11}–Thr^{15}), plus further contacts to O$^{\gamma}$ of Thr^{15}. The ribityl moiety is also stabilized by several hydrogen bonding contacts to backbone and side chain atoms. As can be observed in Table II, a small decrease in the number of hydrogen bonds together with a moderate lengthening of the hydrogen bonds at the phosphate loop may contribute to the reported lower affinity of the mutant complexes relative to wild type (7). On the other hand, the isoalloxazine ring is embedded in the protein, stacked between the aromatic groups Trp^{57} and Tyr^{94} in the wild type structure. It is further stabilized by hydrogen bonds to backbone atoms of segments Gly^{61}–Leu^{62} and Asn^{97}–Gln^{99}. Compared with the wild type flavodoxin, the isoalloxazine-binding site is more accessible to solvent in the W57L mutant (Fig. 2) and similarly accessible in the Y94F one. The ensuing cavity originated in the W57L mutant by the absence of the tryptophan side chain is partially filled through a network of interactions involving three water molecules. The differences between the two mutant holoflavodoxin structures and the wild type one are thus very minor, and in no case did new interactions appear that could complicate the analysis of the kinetic data. We will assume for the purpose of discussion that the rest of the mutants behave similarly and tolerate the introduced mutations without significantly modifying the

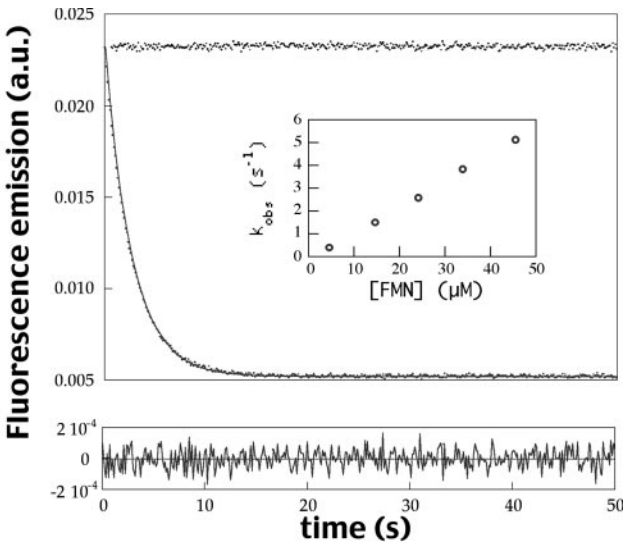

FIG. 3. **Binding of FMN to wild type *Anabaena* apoflavodoxin in 50 mM MOPS, pH 7.0, 25.0 ± 0.1 °C, under pseudo first-order conditions.** Excitation at 445 nm and emission at >500 nm. *Upper panel*, decrease in emission fluorescence upon FMN complexation with apoflavodoxin after fast mixing. The *horizontal line* shows the fluorescence of FMN upon mixing with buffer. *Lower panel*, difference between the experimental trace and the fit to a single exponential equation. The *inset* shows the fitted pseudo first-order apparent association constant as a function of FMN concentration.

structure of the binding site. This is quite likely the case as their spectroscopic properties and their redox potentials are similar to those of wild type (19).

Binding of FMN to Wild Type Apoflavodoxin in 50 mM MOPS, pH 7.0, 25 °C—The time course of the fluorescence decrease associated to the binding of FMN to wild type apoflavodoxin is shown in Fig. 3. The trace can be fitted to a single exponential equation, and the observed initial fluorescence corresponds to that of unbound FMN, which suggests that the entire binding process is being observed. These data together indicate that the binding of FMN to wild type *Anabaena* apoflavodoxin follows a simple two-state mechanism with no intermediates accumulating during the reaction, as was reported for the *Peptostreptococcus*, *Azotobacter*, and *Desulfovibrio* flavodoxins (5, 25). The *inset* in Fig. 3 shows that the observed rate constant is proportional to FMN concentration, when FMN is in excess, and that it passes through the origin. From the slope of this linear dependence, the microscopic k_{on} can be calculated at 1.15 (±0.05) × 10^5 M^{-1} s^{-1} (Table III).

The temperature dependence of the association rate constant has been studied. The Arrhenius plot in Fig. 4 shows the linear dependence expected when no change in reaction mechanism occurs in the temperature range analyzed. At higher temperatures, the plot is no longer linear (not shown), which is very likely due to apoflavodoxin partial unfolding (22). From the plot, we calculate the following transition state thermodynamic parameters: $\Delta H^{\ddagger}$ = +10.9 (±0.2) kcal mol^{-1}, $\Delta S^{\ddagger}$ = +1.34 (±0.02) cal mol^{-1} K^{-1}, and $\Delta G^{\ddagger}$ of + 10.5 (±0.2) kcal mol^{-1}. The transition state for complex formation is thus mainly destabilized in enthalpic grounds.

Rate Constants of FMN Binding to Mutant Apoflavodoxins—The rate constant of binding of the apoflavodoxin-FMN complex has been, additionally, determined for nine flavodoxin mutants (Fig. 5 and Table III). All mutants bind FMN more slowly than wild type (except T15V whose binding is as fast as that of wild type). The kinetics corresponding to the seven mutants where either Tyr^{94} or Trp^{57} at the isoalloxazine-binding site has been replaced are monoexponential, whereas the two mutants where either Thr^{12} or Thr^{15} at the phosphate-binding site was replaced by valines can be best fitted to double exponentials. In these two mutants, the fast phase accounts for 90% total fluorescence change, and its linear dependence of protein concentration, which passes through the origin, has been used to calculate the rate constants reported in Table III. For the mutants at positions 57 and 94, whose binding mechanism seems two-state, k_{off} values have been calculated from the association constants in Table III and the reported equilibrium binding constants (7). In most cases, with the exception of Y94A, the mutations produced only limited changes in the association rate constants. In seven of the nine mutants analyzed, including residues at positions 12, 15, 57, and 94, the association rate constant is only decreased up to 2-fold. Because most of the residues in contact with FMN in the holoflavodoxin have been mutated, these moderate decreases of the rate constants suggest that, in the rate-limiting step of the association of the two molecules, the interactions between the cofactor and specific side chains are significantly weakened relative to the native complex. As for the dissociation rate constants, the effects are larger, and the increases range from 5- to 30-fold (only the minimal Y94F mutation gives rise to a smaller change).

Binding of Riboflavin to Wild Type and Mutant Apoflavodoxin in 50 mM MOPS, pH 7.0, 25 °C—The binding of riboflavin (the FMN precursor lacking the phosphate moiety) to wild type apoflavodoxin has been analyzed similarly to that of FMN. The time course of the fluorescence decrease associated with riboflavin binding is shown in Fig. 6. The reaction with riboflavin is much faster than with FMN, and the trace can also be fitted to a single exponential. Although this is in principle compatible with a simple two-state binding mechanism, Fig. 7 shows that the observed rate constant, although roughly proportional to the concentration of riboflavin (in the concentration range analyzed), does not pass through zero. This is a clear deviation from two-state behavior that has been interpreted in other systems as revealing the formation of an intermediary complex from where the final complex evolves (40–41).

$$a + b \overset{K}{\longleftrightarrow} ab^* \overset{k_2}{\underset{k_{-2}}{\longleftrightarrow}} a - b$$

SCHEME 1

In Scheme 1 the observed rate constant under pseudo first-order conditions is given by Equation 1,

$$k_{obs} = k_{-2} + k_2 K/(1 + K) \qquad \text{(Eq. 1)}$$

According to this mechanism, if a region where the concentration of reagent in excess is low enough to be explored, an overall fit of the observed rate constant *versus* excess reagent concentration allows the calculation of all the constants shown in Scheme 1. In our case, the fluorescence signal in the low concentration region is too weak, and therefore we can only estimate, as follows, a lower limit for k_2. At high excess reagent concentrations (42), the observed pseudo first-order rate constant takes an upper value of $k_2 + k_{-2}$, whereas at low excess reagent concentrations it takes the lower value of k_{-2}. It follows that k_2 must be equal to or greater than the difference between any two values of k_{obs}. The data in Fig. 7 thus indicate that k_2 must be equal to or greater than 40 s^{-1}. In any case, the binding of riboflavin to wild type apoflavodoxin is clearly faster than that of FMN. A direct comparison between the FMN and riboflavin association constants is possible at high ionic strength where the binding of riboflavin becomes two-state (see below). As for the riboflavin complexes with mutant apoflavodoxins at low ionic strength, a similar deviation from two-state behavior is observed as in the wild type complex (Fig. 7).

TABLE III
Association and dissociation rate constants of FMN/apoflavodoxin complexes

Protein	K_{on} [a]	k_{off} [b]	K_d
	$s^{-1}\ M^{-1}$	s^{-1}	nM
Wild type	$1.15\ (\pm0.05) \times 10^5$	$0.30\ (\pm0.07) \times 10^{-4}$	0.26 (±0.06)
Y94A	$2.04\ (\pm0.10) \times 10^3$	$4.26\ (\pm0.88) \times 10^{-4}$	209 (±40)
Y94F	$5.18\ (\pm0.16) \times 10^4$	$0.54\ (\pm0.08) \times 10^{-4}$	1.04 (±0.15)
Y94W	$8.60\ (\pm0.26) \times 10^4$	$2.88\ (\pm0.35) \times 10^{-4}$	3.35 (±0.37)
W57A	$7.84\ (\pm0.45) \times 10^4$	$8.94\ (\pm0.96) \times 10^{-4}$	11.4 (±1.03)
W57F	$6.52\ (\pm0.13) \times 10^4$	$5.43\ (\pm0.39) \times 10^{-4}$	8.33 (±0.49)
W57Y	$5.47\ (\pm0.27) \times 10^4$	$1.84\ (\pm0.06) \times 10^{-4}$	3.36 (±0.11)
W57L	$2.19\ (\pm0.04) \times 10^4$	$1.47\ (\pm0.34) \times 10^{-4}$	6.72 (±0.81)
T12V	$7.16\ (\pm0.43) \times 10^4$		
T15V	$1.23\ (\pm0.07) \times 10^5$		

[a] In 50 mM MOPS, pH 7.0, at 25 ± 0.1 °C. Errors provided by the fitting program.
[b] Calculated from the k_{on} and the data in third column. Errors calculated by propagating the errors in k_{on} and in K_d.
[c] From Ref. 7.

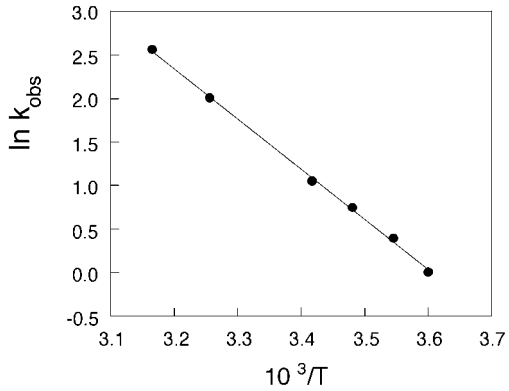

FIG. 4. **Arrhenius plot of the FMN binding to wild type *Anabaena* apoflavodoxin in 50 mM MOPS, pH 7.0, 25.0 ± 0.1 °C.** The concentration of apoflavodoxin and FMN in the mixture were of 0.5 and 40 μM, respectively.

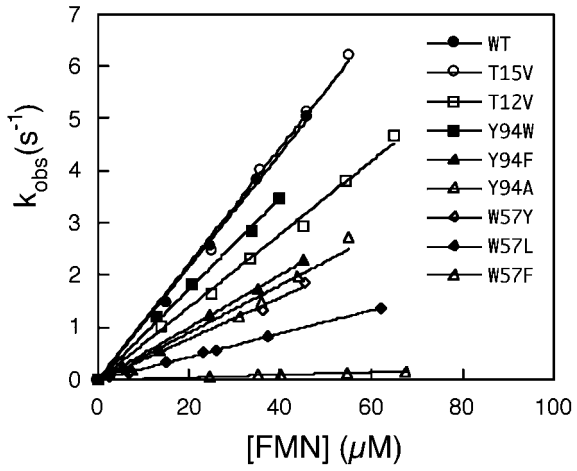

FIG. 5. **Pseudo first-order apparent association constants of FMN binding to apoflavodoxin mutants as a function of FMN concentration.** All experiments performed in 50 mM MOPS, pH 7.0, 25.0 ± 0.1 °C.

Influence of Ionic Strength and of Phosphate on the Binding and Dissociation Rate Constants of the Wild Type Apoflavodoxin-FMN (Riboflavin) Complexes—In an analysis of the apoflavodoxin-FMN complex at equilibrium (7), it was reported that its stability decreases by 0.7 kcal mol^{-1} as the ionic strength is raised from 2 to 500 mM, which reflects the important stabilizing contribution of the charged phosphate group in FMN. However, the binding rate constant of the wild type apoflavodoxin-FMN complex increases as the ionic strength is raised (Fig. 8*A* and Table IV), but this increase is offset by a greater increase of the dissociation rate constant. On going from I = 2 to 500 mM there is a 30-fold increase in k_{on} and a 90-fold increase in k_{off}, resulting in the reported loss of 0.7 kcal mol^{-1}. An increase in binding rate constant with ionic strength for the FMN complexes with *Megasphaera elsdenii* and *Desul-*

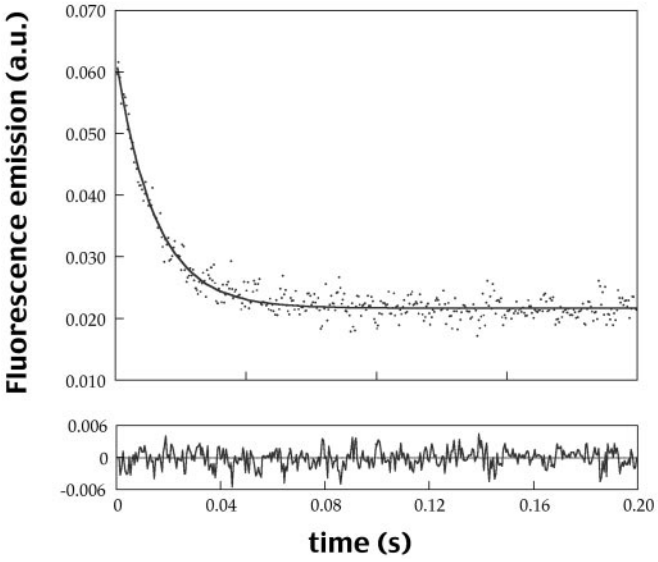

FIG. 6. **Binding of riboflavin to wild type *Anabaena* apoflavodoxin in 50 mM MOPS, pH 7.0, 25.0 ± 0.1 °C, under pseudo first-order conditions.** Excitation at 280 nm and emission at >335 nm. *Upper panel*, decrease in emission fluorescence upon riboflavin complexation with apoflavodoxin after fast mixing. *Lower panel,* difference between the experimental trace and the fit to a single exponential equation.

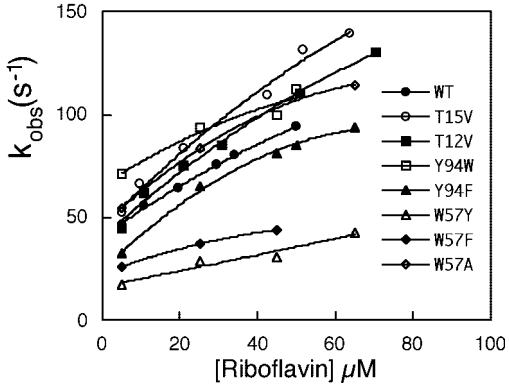

FIG. 7. **Pseudo first-order apparent association constants of riboflavin binding to apoflavodoxin mutants as a function of riboflavin concentration.** All experiments performed in 50 mM MOPS, pH 7.0, 25.0 ± 0.1 °C. The lines are only an aid for the eye.

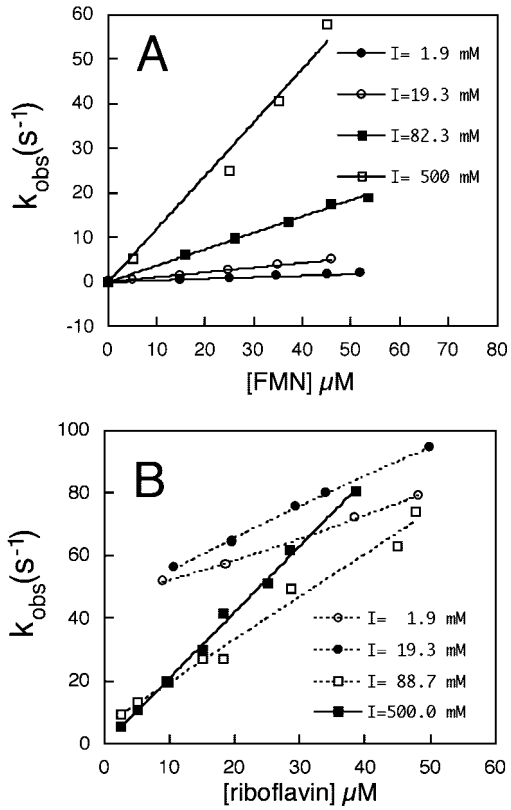

FIG. 8. **Effect of ionic strength on the apparent association constant of the wild type apoflavodoxin complexes with FMN (*A*) and riboflavin (*B*).** Measurements made in 50 mM MOPS, pH 7.0, plus NaCl. The lowest ionic strength (I = 1.9, was achieved in 5 mM MOPS).

fovibrio vulgaris apoflavodoxins has been reported (3, 5, 43). The k_{off} of the *D. vulgaris* complex, however, has been reported to decrease at high ionic strength (5).

In the wild type apoflavodoxin-riboflavin complex, increasing the ionic strength seems to change the binding mechanism so that, at ionic strengths of 89 mM and higher, the extrapolation of the observed rate constants to low riboflavin concentrations goes to zero (Fig. 8*B*). Binding rate constants of 1.7 ($\pm$0.1) $\times$ 10^6 and 2.1 ($\pm$0.2) $\times$ 10^6 s^{-1} M^{-1} are calculated at I = 89 and 500 mM, respectively. At these ionic strengths, the riboflavin rate constants can thus be directly compared with those of FMN confirming that riboflavin binds faster. The riboflavin association rate constants can be combined with the equilibrium binding constants (7) to calculate dissociation rate constants of 3.1 ($\pm$1.4) and 1.2 ($\pm$0.1) s^{-1} at I = 89 and 500 mM, respectively. An increase of k_{on} and a decrease of k_{off} upon increasing ionic strength have also been observed in the riboflavin-*D. vulgaris* apoflavodoxin complex (5).

Additionally, the effect of phosphate concentration on the association rate constants of the wild type apoflavodoxin complexes with FMN and riboflavin has been examined at a constant ionic strength of 500 mM (Table V). Phosphate only slightly decreases the association rate constant of the FMN complex and has no effect on the binding of riboflavin.

DISCUSSION

Structural Insight on the Transition State of Binding from Φ *Analysis*—Φ analysis of protein conformations (27) is a powerful tool to obtain structural information of protein folding transition states (44), transient folding intermediates (45), transition states of complex unfolding (46), transition states of complex formation (47), and equilibrium intermediates (22). In the analysis of transition states of complex formation the idea is to perturb the complex by performing mutations and to quantify the effects in the ground state and transition state complexes. For an analysis based in point mutations, a Φ parameter can be defined as shown in Equations 2 and 3,

$$\phi = \Delta\Delta G^{\ddagger}/\Delta\Delta G_b \quad \text{(Eq. 2)}$$

where

$$\Delta\Delta G^{\ddagger} = -RT\,In(k_{on}\text{wt}/k_{on}\text{mut}) \quad \text{(Eq. 3)}$$

When an interaction between protein and ligand is similarly formed in the ground and transition state complexes, its mutational perturbation will alter the complexes strengths similarly, and the value of the Φ parameter will be 1. If, however, the perturbation is introduced in a residue that does not interact with the ligand in the transition state, then only the stability of the ground state will change and the Φ parameter will have a value of 0. Intermediate Φ values can reflect partial formation of the probed protein/ligand interaction in the transition state or a variety of transient conformations. To derive Φ values, both the equilibrium binding constants and the rate constants of binding are required. The binding rate constants of the wild type and mutant apoflavodoxin-FMN complex are summarized in Table III. The corresponding equilibrium constants are from Ref. 7.

Table VI shows several differential binding energies (wild type minus mutant) of the ground and transition state FMN-apoflavodoxin complex and their associated Φ values. The highest Φ values are those involving the Tyr^{94} residue. This highly conserved tyrosine plays a major role in shaping the redox potentials of flavodoxin (19), and its contribution to the binding of the isoalloxazine ring in the ground state complex is the largest so far attributed to a single residue (7). We have analyzed here two bigger-to-smaller mutations at position 94 (Y94A and Y94F) and one smaller-to-bigger one (Y94W). Mutating the tyrosine to alanine greatly destabilizes the ground complex. This profound destabilization is also manifested in the transition state complex, and a Φ value of 0.6 is obtained. The most likely explanation is that the FMN is already interacting with Tyr^{94} in the transition state of complex formation, although the interaction is not completely native (one can speculate that the very close contact between the flavin and tyrosine aromatic rings that is observed in the ground state complex (holoflavodoxin) is not fully established yet or perhaps that the orientation of the rings is not the most favorable one). Interestingly, the Y94F mutant (whose x-ray structure is shown here to be virtually identical to that of wt) gives rise to essentially the same Φ value of 0.6 despite the fact that the destabilization of the ground and transient complexes is much smaller than in Y94A, which confirms that the FMN is interacting significantly with the residue at position 94 in the transition state. The Φ value when position 94 is probed with a tryptophan residue is much lower (0.12). In this case, however, the introduced side chain is bigger that the wild type tyrosine, and the possibility exists that the transient complex, if not the ground state one, is different from that observed in wild type and mutants where position 94 has been shortened. The averaged Φ value at position 94 is calculated at 0.44.

The substitutions studied at position 57 are, in all cases, to smaller residues than the wild type tryptophan. The contribution of Trp^{57} to shape the redox potentials in flavodoxin is only moderate (19). It makes nevertheless an important contribution to the stability of the apoflavodoxin-FMN complex, although not as large as that of Tyr^{94} (7). Trp^{57} is conserved among flavodoxins but not as much as Tyr^{94}. The Φ values measured at position 57 are lower than at position 94 (Table

TABLE IV
Effect of ionic strength on the association and dissociation rate constants of the wild-type apoflavodoxin-FMN complex

Ionic strength	k_{on} [a]	k_{off} [b]	K_d [ac]
mM	$M^{-1}\ s^{-1}$	s^{-1}	nM
1.9	$3.94\ (\pm0.08) \times 10^4$	$7.65\ (\pm4.78) \times 10^{-6}$	0.194 (±0.121)
19.3	$1.15\ (\pm0.02) \times 10^5$	$30.4\ (\pm2.2) \times 10^{-6}$	0.264 (±0.060)
82.5	$3.50\ (\pm0.07) \times 10^5$	$164\ (\pm36) \times 10^{-6}$	0.470 (±0.026)
500.0	$1.30\ (\pm0.14) \times 10^6$	$691\ (\pm209) \times 10^{-6}$	0.532 (±0.102)

[a] Measurements were made in 50 mM, MOPS, pH 7.0, containing NaCl, except for third column, made in 5 mM MOPS, at 25 ± 0.1 °C. Errors provided by the fitting program.
[b] Calculated from the k_{on} and the data in third column. Errors calculated by propagating the errors in k_{on} and in K_d.
[c] Data from Ref. 7.

TABLE V
Effect of phosphate concentration (at constant ionic strength) on the association rate constants for the wild-type apoflavodoxin-FMN and apoflavodoxin-riboflavin complexes

[Phosphate]	k_{on} [a]	
	FMN	Riboflavin
	$M^{-1}\ s^{-1}$	
0	$13.0\ (\pm1.4) \times 10^5$	$2.11\ (\pm0.11) \times 10^6$
1	$6.44\ (\pm0.32) \times 10^5$	$2.04\ (\pm0.12) \times 10^6$
10	$6.89\ (\pm0.28) \times 10^5$	$2.01\ (\pm0.08) \times 10^6$
100	$4.82\ (\pm0.29) \times 10^5$	$2.05\ (\pm0.12) \times 10^6$

[a] Measurements at 25 ± 0.1 °C in 50 mM MOPS, pH 7.0, plus NaCl to set a constant ionic strength of 500 mM. Errors provided by the fitting program.

TABLE VI
ϕ analysis of the apoflavodoxin-FMN complex transition state

Protein	$\Delta\Delta G^{\ddagger}_{+}$ [a]	$\Delta\Delta G_b$ [b]	ϕ [c]
Y94A	−2.38 (±0.05)	−4.00 (±0.14)	0.60 (±0.02)
Y94F	−0.47 (±0.06)	−0.80 (±0.14)	0.59 (±0.13)
Y94W	−0.17 (±0.03)	−1.50 (±0.14)	0.12 (±0.02)
W57A	−0.23 (±0.04)	−2.27 (±0.11)	0.10 (±0.02)
W57F	−0.33 (±0.03)	−2.08 (±0.10)	0.16 (±0.02)
W57Y	−0.44 (±0.04)	−1.55 (±0.10)	0.28 (±0.03)
W57L	−0.98 (±0.03)	−2.00 (±0.14)	0.49 (±0.04)
T12V	−0.28 (±0.04)	−3.88 (±0.10)	0.07 (±0.01)
T15V	0.04 (±0.04)	−1.73 (±0.10)	−0.02 (±0.02)

[a] Calculated as $-RT$ ln (k_{on} wt/k_{on}mut) using data in Table III, with error propagation.
[b] Data from Ref. 7.
[c] $\phi = \Delta\Delta G^{\ddagger}/\Delta\Delta G_b$. Errors calculated by propagating the errors in $\Delta\Delta G^{\ddagger}$ and $\Delta\Delta G_b$.

VI). They range from 0.10 for the WA mutation to 0.49 for the WL one. The average Φ value at position 57 is 0.26, reflecting a non-negligible but small interaction between the FMN and Trp^{57} in the transition state complex.

The last region investigated corresponds to the phosphate-binding site. Although many of the interactions established by the FMN phosphate with apoflavodoxin are with main chain hydrogen bond donors (16), it also forms hydrogen bonds with threonine side chains that can be conveniently mutated. We use threonine to valine mutations because these residues are isosteric and because the full disruption of hydrogen bonds with the phosphate group, presumably not compensated with new hydrogen bonds with solvent, is likely to produce large energy differences that are convenient to derive reliable Φ values. The values obtained for the two mutations analyzed (Table VI) indicate that the phosphate moiety in FMN is not in contact with either Thr^{12} or with Thr^{15} in the transition state complex. As the other groups forming the phosphate-binding site are located in the neighborhood of these threonines (Fig. 1), it seems reasonable to interpret this result as indicating that the phosphate is not docked into its binding site in the transition state of complex formation.

Salt and Phosphate Effects and the Faster Binding of Riboflavin—The preliminary picture emerging from the Φ analysis is that of a transition state complex where the FMN is significantly bonded to Tyr^{94}, weakly bonded to Trp^{57}, and not bonded at the phosphate-binding site. One such complex would be stabilized by hydrophobic interactions between the FMN and Tyr^{94} (and to a lesser extent Trp^{57}), whereas polar interactions between the charged phosphate and its binding site should be negligible. This is in contrast with the holoflavodoxin ground state complex that is destabilized by high ionic strength, showing the importance of polar interactions (7).

The observed salt effect on the binding and dissociation rate constants (Table IV) is fully consistent with this scenario. Increasing the ionic strength markedly raises both the rates of binding and dissociation. The increase in the binding rate constant (33-fold from I = 1 to 500 mM) derives from a strengthening of the hydrophobic interactions that appear in the transition state complex upon interaction of the dissociated molecules. At high ionic strength, our data indicate (Fig. 9) that the energy of the transition state is lowered relative to that of the interacting molecules by 2.1 kcal mol^{-1} (incidentally, for similar reasons the strength of the ground state apoflavodoxin-riboflavin complex is increased by 2.6 kcal mol^{-1}, going from I = 2 to I = 500 mM (7)). On the other hand, the salt effect on the dissociation rate constant (a 91-fold increase from I = 1 to 500 mM) is due to the fact that the polar interactions established by the FMN phosphate moiety in the ground state complex (but not in the transition state one) are markedly weakened by salt. From the 91-fold increase in dissociation rate constant, we calculate that the energy gap between the ground state complex and the transition state one is decreased by 2.7 kcal mol^{-1} at high ionic strength, thus lowering the dissociation activation barrier. Because the hydrophobic interactions in the ground state are also strengthened at high salt, the net destabilization of the ground state complex by high ionic strength is small (Fig. 9 and Ref. 7).

The observed phosphate effect on the binding constant is also consistent because it is a rather small effect (Table V) hardly compatible with the apoflavodoxin phosphate-binding site playing a prominent role in the stabilization of the transition state complex. The effect could simply arise from a lower efficiency of FMN collisions in the presence of bound phosphate, due to steric reasons or to an electrostatic repulsion with the phosphate in FMN.

Finally, the faster binding of riboflavin compared with FMN (despite its much lower affinity (7)) is also in agreement with the binding of FMN starting at the isoalloxazine-binding site. To initiate a binding event at a hydrophobic pocket, a smaller uncharged molecule such as riboflavin seems better suited than a larger charged one such as FMN. In this respect, the extra phosphate in FMN can only decrease the efficiency of collisions at the isoalloxazine-binding site. On the other hand, if the interaction between FMN and apoflavodoxin had to begin at the phosphate site (so as to either increase the apparent concentration of FMN near the apoprotein or in order to drive a conformational change that opened an otherwise closed

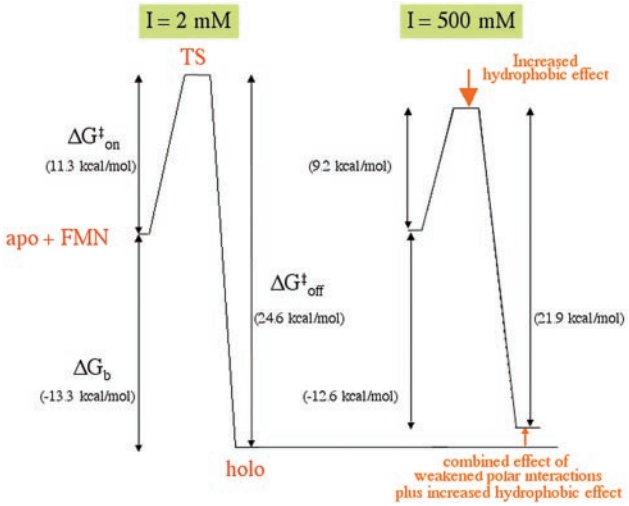

FIG. 9. **Free energy diagrams of the ground and transition state apoflavodoxin-FMN complexes at low and high ionic strengths showing the effects of the ionic strength on the stability of the complexes.** Hydrophobic interactions between Trp^{57} and Tyr^{94}, and the FMN isoalloxazine are strengthened in both complexes, but in the ground state complex, this is more than compensated for by a weakening of polar interactions between the phosphate and the protein, which leads to a lower stability. Both the kinetic association and dissociation constants are increased by increasing the ionic strength (see text).

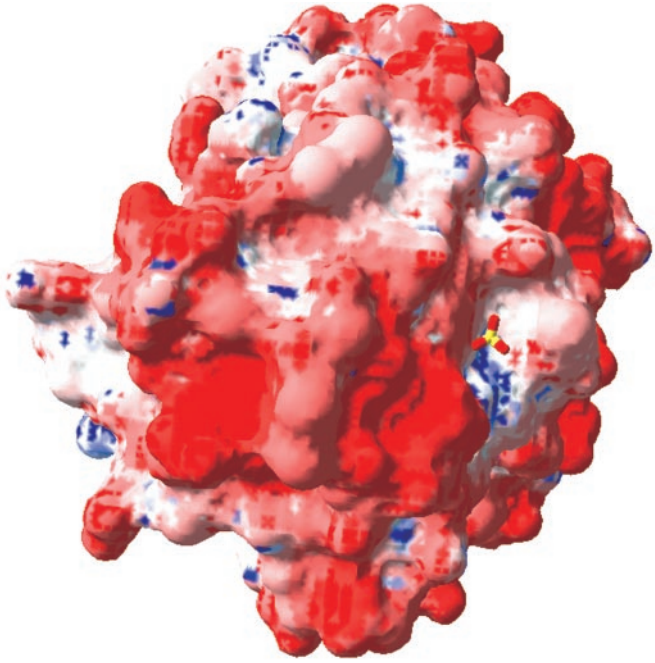

FIG. 10. **Electrostatic potential surface of *Anabaena* apoflavodoxin (Protein Data Bank code 1ftg) (calculated with Swiss-pdbviewer after having removed the bound sulfate anion), showing the sulfate as it is bound to the apoflavodoxin structure (Protein Data Bank code 1ftg).** The surface has been calculated using partial changes and the Poisson-Boltzmann equations, using water and protein dielectric constants of 80 and 4, respectively, and a solvent ionic strength of 0 M. This sulfate mimics the binding of the phosphate in FMN.

isoalloxazine site as is observed in the crystal structure (17)), one would expect FMN to bind faster than riboflavin, which is not the case.

Mechanism of Binding—All the analyses performed over the years on different flavodoxins indicate that most of the binding energy of the complex derives from interactions of the isoalloxazine and of the phosphate moieties with the apoprotein, the ribityl contributing little to the stability (1). A simple inspection of flavodoxin structures allows an easy interpretation of this fact because the ribityl forms less interactions; it is more solvent-exposed, and unlike those of the other FMN moieties, its binding site is not conserved among flavodoxins. It thus follows that an important role in the kinetics of complex formation has to be attributed either to the phosphate or to the isoalloxazine. Although a binding starting at the isoalloxazine site fits well with the view where nonspecific interactions such as the hydrophobic effect can drive an efficient encounter of protein/ligand molecules, there is much recent evidence (48–53) indicating that some proteins use electrostatic attraction to accelerate ligand binding. In the case of flavodoxins this should occur by attracting the phosphate moiety of FMN. It should be noticed, however, that the interaction between FMN phosphate and apoflavodoxin does not rely in positively charged residues but in just hydrogen bonding (16). In addition, the apoflavodoxin potential energy surface (Fig. 10) shows that the phosphate-binding site is not well suited to attract anions at a distance. Although a small positive region, mainly due to unpaired NH groups is close, the overall potential in the phosphate-binding site is negative (as expected of a highly acidic protein such as flavodoxin). A second line of evidence that could in principle point to the phosphate site as the kinetically important binding spot derives from inspection of the x-ray structure of *Anabaena* apoflavodoxin (17). In this structure, the phosphate-binding site (which bears a bound sulfate anion) appears to be in the same conformation as in holoflavodoxin, whereas the isoalloxazine-binding site is closed because Trp^{57} has flipped toward Tyr^{94}. It seems that only the phosphate can interact with apoflavodoxin without a conformational change taking place. It is unfortunate that, despite the efforts devoted to solving both the *Azotobacter* (26) and the *Anabaena* (20) structures, no full solution structure of an apoflavodoxin is available so far. However, the NMR data gathered on these proteins, in the absence of a bound anion (20, 26), clearly indicate that the phosphate-binding site is quite flexible or disordered and that the apparently well packed closed isoalloxazine-binding site is quite flexible (probably due to flexibility of the loop bearing Trp^{57}, which is evident when different x-ray structures are compared (7)). There is thus no conclusive reason to consider that, in solution, the phosphate site is closer to its native conformation than the isoalloxazine site.

Because neither the x-ray structure nor the electrostatic potential surface can help to elucidate where the binding of FMN starts, kinetic studies are required. More specifically, a kinetic analysis of apoflavodoxin mutants seems the most promising approach. The Φ analysis performed on mutants located at the two binding spots (the phosphate- and the isoalloxazine-binding sites) clearly points to the isoalloxazine site as the region where the interaction between the FMN and apoflavodoxin is formed to a greater extent in the rate-limiting step of binding. Because the observed association process seems to be a two-state process, this is strong evidence supporting that the complex starts by interaction of the isoalloxazine with its binding site and that this interaction appears to be formed to a greater extent with Tyr^{94} than with Trp^{57}. The Φ analysis also indicates that the phosphate is not interacting with any of the two hydrogen-bonding groups that have been probed at its site, which suggests the phosphate is not docked at all in the transition state complex. Although an interpretation of the transition state enthalpy and entropy change is difficult, the significant enthalpy value found for the FMN complex may be reflecting that a partial desolvation of the phosphate has to occur in order for the FMN to interact at the isoalloxazine site, although other reasons could be invoked

such as an electrostatic repulsion from the negative field of apoflavodoxin or a rearrangement of binding site residues. The small activation entropy points to a compensation of translational and rotational entropy lost and the hydrophobic effect already manifested in the transition state complex.

A second line of evidence supporting the proposed mechanism comes from the fact that riboflavin, which lacks the phosphate moiety in FMN, binds generally faster than FMN to the *Anabaena* as well as to the other apoflavodoxins studied (2, 5, 25), despite the lower affinity of the riboflavin-apoflavodoxin complex. In addition, the fairly small phosphate effect on the rate of FMN binding (compared with the much larger effect of the ionic strength) is consistent with the binding of FMN starting at the isoalloxazine site, since a much more marked inhibition would be expected in the presence of 0.1 M phosphate if the rate-limiting step were at the interaction of FMN at the phosphate site. A third piece of supporting evidence derives from the observed ionic strength effect on the rate constants of FMN association and dissociation. If the binding of FMN starts at the isoalloxazine site, the expected salt effects are precisely those that are observed, an acceleration of both the rate constants of binding and of dissociation. An initial binding at the phosphate site, on the contrary, would lead to a concomitant slower binding at high ionic strength.

All the evidence thus leads us to conclude that FMN initiates its binding to apoflavodoxin by partial docking of the isoalloxazine moiety at the hydrophobic binding site formed by Tyr^{94} and Trp^{57}, without a significant participation of the phosphate site. In the end, it seems reasonable for a negatively charged molecule to approach a negatively charged protein by using hydrophobic interactions and then to stabilize the negative charge by establishing appropriate local hydrogen bonding interactions. It is possible that this strategy be shared with other acidic proteins that form complexes with amphipathic anionic ligands.

Protein Data Bank Accession Numbers—The coordinates for the final models have been deposited in the Protein Data Bank under the ID codes 1obo and 1obv, for W57L and Y94F flavodoxin, respectively.

Acknowledgment—We thank the staff of beamlines X11 and X31 at DESY (Hamburg, Germany) for support.

REFERENCES

1. Müller, F. (ed) (1992) *Chemistry and Biochemistry of Flavoenzymes*, CRC Press, Inc., Boca Raton, FL
2. Edmondson, D. E., and Tollin, G. (1971) *Biochemistry* **10,** 124–132
3. Mayhew, S. G. (1971) *Biochim. Biophys. Acta* **235,** 289–302
4. Mayhew, S. G., and Tollin, G. (1992) in *Chemistry and Biochemistry of Flavoenzymes* (Müller, F., ed) Vol. III, pp. 389–426, CRC Press, Inc., Boca Raton, FL
5. Pueyo, J. J., Curley, G. P., and Mayhew, S. G. (1996) *Biochem. J.* **313,** 855–861
6. Druhan, L. J., and Swenson, R. P. (1998) *Biochemistry* **37,** 9668–9678
7. Lostao, A., El Harrous, M., Daoudi, F., Romero, A., Parody-Morreale, A., and Sancho, J. (2000) *J. Biol. Chem.* **275,** 9518–9526
8. Smoluchowski, M. V. (1917) *Z. Phys. Chem.* **92,** 129–168
9. Berg, O. G., and von Hippel, P. H. (1985) *Annu. Rev. Biophys. Biophys. Chem.* **14,** 131–160
10. Nortrup, S. H., and Erickson, H. P. (1992) *Proc. Natl. Acad. Sci. U. S. A.* **89,** 3338–3342
11. Selzer, T., and Schreiber, G. (1999) *J. Mol. Biol.* **287,** 409–419
12. Wade, R. C., Luty, B. A. Demchuk, E. D., Madura, J. D., Davis, M. E., Briggs, J. M., and McCammon, J. A. (1994) *Nat. Struct. Biol.* **1,** 65–69
13. Schreiber, G., and Fersht, A. R. (1996) *Nat. Struct. Biol.* **3,** 427–431
14. Scheinerman, F. B., Norel, R., and Honig, B. (2000) *Curr. Opin. Struct. Biol.* **10,** 153–159
15. Selzer, T., Albeck, S., and Schreiber, G. (2000) *Nat. Struct. Biol.* **7,** 537–541
16. Rao, S. T., Shaffie, F., Yu, C., Satyshur, K. A., Stockman, B. J., Markley, J. L., and Sundaralingan, M. (1992) *Protein Sci.* **1,** 1413–1427
17. Genzor, C. G., Perales-Alcón, A., Sancho, J., and Romero, A. (1996) *Nat. Struct. Biol.* **3,** 329–332
18. Genzor, C. G., Beldarraín, A., Gómez-Moreno, C., López-Lacomba, J. L., Cortijo, M., and Sancho, J. (1996) *Protein Sci.* **5,** 1376–1388
19. Lostao, A., Gómez-Moreno, C., Mayhew, S. G., and Sancho, J. (1997) *Biochemistry* **36,** 14334–14344
20. Langdon, G. M., Jimenez, M. A., Genzor, C. G., Maldonado, S., Sancho, J., and Rico, M. (2001) *Proteins* **43,** 476–488
21. Fernández-Recio, J., Genzor, C. G., and Sancho, J. (2001) *Biochemistry* **40,** 15234–15245
22. Irún, M. P., Garcia-Mira, M. M., Sanchez-Ruiz, J. M., and Sancho, J. (2001) *J. Mol. Biol.* **306,** 877–888
23. Maldonado, S., Irún, M. P., Campos, L. A., Rubio, J. A., Luquita, A., Lostao, A., Wang, R., García-Moreno, B., and Sancho, J. (2002) *Protein Sci.* **11,** 1260–1273
24. Casaus, J. L., Navarro, J. A., Hervas, M., Lostao, A., De La Rosa, M. A., Gomez-Moreno, C., Sancho, J., and Medina, M. (2002) *J. Biol. Chem.* **277,** 22338–22344
25. Gast, R., and Müller, F. (1978) *Helv. Chim. Acta* **61,** 1353–1363
26. Steensma, E., and van Mierlo, C. P. (1998) *J. Mol. Biol.* **282,** 653–666
27. Fersht, A. R., Matouschеck, A., and Serrano, L. (1992) *J. Mol. Biol.* **224,** 771–782
28. Fillat, M. F., Borrias, W. E., and Weisbeerk, P. J. (1991) *Biochem. J.* **280,** 187–191
29. Deng, W. P., and Nickoloff, J. A. (1992) *Anal. Biochem.* **200,** 81–88
30. Gill, S. C., and von Hippel, P. H. (1989) *Anal. Biochem.* **182,** 319–326
31. Jankarik, J., and Kim, S. J. H. (1991) *J. Appl. Crystallogr.* **24,** 409–411
32. Biertümpfel, C., Basquin, J., Suck, D., and Sauter, C. (2002) *Acta Crystallogr. Sect. D Biol. Crystallogr.* **58,** 1657–1659
33. Collaborative Computer Project No. 4 (1994) *Acta Crystallogr. Sect. D Biol. Crystallogr.* **50,** 760–763
34. Navaza, J. (1994) *Acta Crystallogr. Sect. A* **50,** 157–163
35. Smith, W. W., Pattridge, K. A., Ludwig, M. L., Petsko, G. A., Tsernoglou, D., Tanaka, M., and Yasunobu, K. T. (1983) *J. Mol. Biol.* **165,** 737–755
36. Fukuyama, K., Wakabayashi, S., Matsubara, H., and Rogers, L. J. (1990) *J. Biol. Chem.* **265,** 15804–15812
37. Watt, W., Tulinsky, A., Swenson, R. P., and Watenpaugh, K. D. (1991) *J. Mol. Biol.* **218,** 195–208
38. Ludwig, M. L., and Luschinsky, C. L. (1992) in *Chemistry and Biochemistry of Flavoenzymes* (Müller, F., ed) Vol. III, pp. 427–466, CRC Press, Inc., Ann Arbor, MI
39. Freigang, J., Diederichs, K., Schafer, K. P., Welte, W., and Paul, R. (2002) *Protein Sci.* **11,** 253–261
40. Dumotier, C., Gorbunoff, M. J., Andreu, J. M., and Engelborghs, Y. (1996) *Biochemistry* **35,** 4387–4395
41. Díaz, J. F., Strobe, R., Engelborghs, Y., Souto, A. A., and Andre, J. M. (2000) *J. Biol. Chem.* **275,** 26265–26276
42. Fierke, C. A., and Hammes, G. G. (1995) *Methods Enzymol.* **249,** 3–37
43. Gast, R., Valk, B. E., Müller, F., Mayhew, S. G., and Veeger, C. (1976) *Biochim. Biophys. Acta* **446,** 463–471
44. Matouschek, A., Kellis, J. T., Jr., Serrano, L., and Fersht, A. R. (1989) *Nature* **340,** 122–126
45. Matouschek, A., Kellis, J. T., Jr., Serrano, L., Bycroft, M., and Fersht, A. R. (1990) *Nature* **346,** 440–445
46. Sancho, J., Meiering, E. M., and Fersht, A. R. (1991) *J. Mol. Biol.* **221,** 1007–1014
47. Schreiber, G., and Fersht, A. R. (1995) *J. Mol. Biol.* **248,** 478–486
48. Perrett, S., Zahn, R., Stenberg, G., and Fersht, A. R. (1997) *J. Mol. Biol.* **269,** 892–901
49. Wade, R. C., Gabdoulline, R. R., Ludemann, S. K., and Lounnas, V. (1998) *Proc. Natl. Acad. Sci. U. S. A.* **95,** 5942–5949
50. Baerga-Ortiz, A., Rezaie, A., and Komives, E. A. (2000) *J. Mol. Biol.* **296,** 651–658
51. Frisch, C., Fersht, A. R., and Schreiber, G. (2001) *J. Mol. Biol.* **308,** 69–77
52. Gabdoulline, R. R., and Wade, R. C. (2001) *J. Mol. Biol.* **306,** 1139–1155
53. Gabdoulline, R. R., and Wade, R. C. (2002) *Curr. Opin. Struct. Biol.* **12,** 204–213
54. Sheldrick, G. M., and Schneider, T. R. (1997) *Methods Enzymol.* **277,** 319–343
55. Brunger, A. T., Adams, P. D., Clore, G. M., DeLano, W. L., Gros, P., Grosse-Kunstleve, R. W., Jiang, J.-S., Kuszewski, J., Nilges, N., Pannu, N. S., Read, R. J., Rice, L. M., Simonson, T., and Warren, G. L. (1998) *Acta Crystallogr. Sect. D Biol. Crystallogr.* **54,** 905–921